Syntectonic carbonation during synmagmatic mantle exhumation at an ocean-continent transition

Rémi Coltat, Philippe Boulvais, Yannick Branquet, J. Collot, M.E. Epin, G. Manatschal

Publisher: GSA
Journal: GEOL: Geology
DOI:10.1130/G45530.1

Syn-tectonic carbonation during syn-magmatic mantle exhumation at an ocean-continent transition

Rémi Coltat[1], P. Boulvais[1], Y. Branquet[1,2], J. Collot[1], M.E. Epin[3], and Gianreto Manatschal[3]

[1]*Université Rennes, CNRS, Géosciences Rennes, UMR 6118, F-35000 Rennes, France*

[2]*Institut des Sciences de la Terre d'Orléans, UMR 7327, Université Orléans, 45234 Orléans, France*

[3]*Institut de Physique du Globe de Strasbourg, EOST-CNRS UMR 7516, Université Strasbourg, 67084 Strasbourg, France*

ABSTRACT

A Jurassic extensional detachment associated with carbonated serpentinites and basalts is preserved at Falotta (Platta nappe, southeastern Switzerland). Structural data indicates that fluid circulation occurred during late increments of extension along the detachment plane, separating serpentinites from basalts. The homogeneity of the isotopic signatures ($\delta^{18}O$ ~16‰ and $\delta^{13}C$ centered on 0–1‰) can be best explained by a single, sudden seawater-derived carbonation event at temperatures of ~100 °C. Carbonation was focused in the high permeability zone along the detachment. Our model yields new insights for carbonation processes related to mantle exhumation.

INTRODUCTION

An important discovery in the study of passive margins was the recognition of extensional detachments and mantle exhumation in the most distal parts of magma-poor systems (Boillot et al., 1987). These structures resemble oceanic detachments that have

Publisher: GSA
Journal: GEOL: Geology
DOI:10.1130/G45530.1

been observed at mid-ocean ridges (MacLeod et al., 2002; Cannat et al., 2009). MacLeod et al. (2002) showed that large volumes of seawater interacted with the exhuming mantle resulting in serpentinization of the uppermost 6 km of the exhumed mantle domain. While hydrothermal cells lead to mineralization in the exhumed mantle (~1–3 km; McCaig et al., 2007), ophicalcites develop within serpentinites close to the seafloor (Weissert and Bernoulli, 1984). Characterizing such shallow fluid-rock interactions is necessary to understand the chemical exchanges between the mantle and seawater reservoirs and the mass budgets involved in metal deposition (Fe, Cu, Zn) close to or at the seafloor.

In this paper, we present structural and geochemical data on the carbonation associated with a well-preserved extensional detachment system exposed at Falotta in the Platta nappe (southeastern Switzerland). We show that syn-tectonic carbonation occurred during syn-magmatic mantle exhumation.

GEOLOGICAL SETTING

The Platta nappe, exposed in the southeastern Swiss Alps, hosts remnants of the Jurassic Alpine Tethys Ocean Continent Transition (OCT; Fig. 1A). East-west–directed regional extension, accommodated along mantle detachment faults (Desmurs et al., 2001), was accompanied by mafic magmatism dated at 161 Ma (Schaltegger et al., 2002). The Platta nappe is primarily composed of serpentinized mantle rocks and mafic rocks. The serpentinites are carbonated at their paleo-surface, forming fracture-filling ophicalcites (terminology of Bernoulli and Weissert, 1985). Tectono-sedimentary carbonated mantle breccias (ophiolite breccias of Bernoulli and Weissert, 1985) occur above the exhumed mantle. Mafic volcanic rocks (hyaloclastites, pillows, and lava flows)

Publisher: GSA
Journal: GEOL: Geology
DOI:10.1130/G45530.1

overlie the ophicalcites. The exhumed mantle rocks, breccias and basalts are capped by the Radiolarian Chert Formation dated between 166 and 147 Ma (Bill et al., 2001).

PETROGRAPHIC AND STRUCTURAL DATA

At Falotta, three lithological units can be distinguished that are from bottom to top: serpentinites, ophicalcites, and basalts (Figs. 1B, 2A, and 3A). The serpentinites consist of cataclasites with preserved serpentinite lenses crosscut by green serpentine veins, gradually evolving upwards to a fault gouge (see also Picazo et al., 2013; Pinto et al., 2015). The ophicalcites consist of, from bottom to top, (1) fracture-filling ophicalcites with veins of fibrous calcite, and (2) foliated ophicalcites. The latter consist of large anastomosing and foliated carbonate shear bands (SBs) developed in serpentinite breccias and around preserved lenses of various sizes (Fig. 2A). The sub-horizontal foliation, broadly N°20 in strike, is defined by actinolite, carbonate, and minor talc and chlorite. Carbonate veins mimic the foliation. The basalt unit contains foliated hyaloclastites, foliated basalts, veined basalts and massive basalts further up-section (Figs. 2A and 3A). The foliation is defined by amphibole and chlorite and displays the same strikes and dips as those observed in the foliated ophicalcites. The basalts are extensively epidotized and chloritized along ribbons near the base.

Whereas carbonation may be locally massive and pervasive, replacing serpentinite clasts and matrix, it is expressed throughout the whole section by veins and shear bands (Fig. 3A). Only calcite, white to greyish in color, is observed. The extensional or hybrid shear extensional character of the veins is indicated by fibrous habits of calcite filling and wall rock offsets with calcite being the latest phase to crystallize (Figs. 2B–2E). Extensional veins (EVs) in the serpentinites and ophicalcites contain coarse calcite (up to

several millimeters) and minor amphibole and chlorite at their rims. The EVs crosscut the serpentine veins (Fig. 2B). In the basalts, veins consisting of epidote, quartz, chlorite, and albite, defining a greenschist paragenesis, are filled by late calcite (Fig. 2C). Hybrid shear extensional veins (SVs) in the serpentinites and ophicalcites are filled with tiny calcite (~10–50 µm) and actinolite. Close to the contact with the basalts talc and hydro-andradite (garnet composition specified by scanning electron microscopy [SEM] analyses) are found in veins. In the basalts, sparitic to micro-sparitic calcite is associated with actinolite, iron oxides, talc, and hydro-andradite. Calcitic shear bands found in the serpentinites and ophicalcites are composed of tiny calcite, actinolite, and minor chlorite, leaving clasts made of serpentinite, serpentine, pyroxene, spinel, and magnetite. Within the shear bands, the lack of dynamic recrystallization of the carbonate grains and the cracks found in the grains argue for a cataclastic fabric (Fig. 2D). Locally, jogs between calcitic shear veins form pull-apart structures filled with fibrous calcite (Fig. 2E).

Vein orientations and dips are plotted in Figure 3B. Throughout the section, calcite fibers are sub-horizontal and oriented east-west. SVs dip ~40–50° either to the east or to the west, whereas EVs steeply dip ~70–80°. At the base of the fracture-filling ophicalcites, SVs strike N°160, whereas EVs have an N°0 orientation on average (Fig. 3B). EVs at the top of the fracture-filling ophicalcites trend N°160. In the foliated ophicalcites, SVs and EVs roughly trend N°30 (Fig. 3B). In the basalts, EVs are N°30 and SVs trend N°40.

STABLE ISOTOPE COMPOSITIONS

The $\delta^{18}O$ and $\delta^{13}C$ values of calcite are homogenous throughout the section with no significant differences for the different types of veins and shear bands (Fig. 3C,

Publisher: GSA
Journal: GEOL: Geology
DOI:10.1130/G45530.1

Appendix DR2 in the GSA Data Repository[1]). The $\delta^{18}O$ values are centered at ~16.0‰ ± 0.3‰ (with a range of 15.4–17.0‰). The $\delta^{13}C$ values are slightly more dispersed with values between –0.44‰ and +2.12‰.

DISCUSSION

Jurassic Carbonation from Seawater

A recurring problem when dealing with Jurassic extensional events in the European Alps is to assess the importance of the Alpine overprint (Weissert and Bernoulli, 1984; Früh-Green et al., 1990). There are several arguments for a Jurassic carbonation from seawater, with no Alpine deformation and metamorphic overprint nor isotopic resetting.

(1) Sub-vertical calcitic veins with east-west sub-horizontal fibers, together with conjugate hybrid shear extensional veins with normal sense of shear, are indicative of horizontal stretching/extension during carbonation. Normal shear bands in foliated ophicalcites and conjugate hybrid shear extensional veins are symmetric systems diagnostic of coaxial strain. These features, together with the lack of reverse shears on the outcrop (Fig. 2A), are compatible with extensional deformation rather than Alpine thrusting. Notably the structural pattern of veining is similar to veining associated with slip along detachment faults (e.g., Mehl et al., 2005).

(2) The overall east-west extension during Jurassic exhumation is consistent with the orientations of carbonate veins and fibers documented here (Froitzheim and Manatschal, 1996).

Publisher: GSA
Journal: GEOL: Geology
DOI:10.1130/G45530.1

(3) The presence of hydro-andradite suggests precipitation during oceanic hydrothermalism rather than during regional Alpine metamorphism (Gutzmer et al., 2001).

(4) One would expect that calcite crystals with variable habits (small versus large veins, minute veins versus pluri-metric ophicalcitized zones, veins hosted in basalts and serpentinites) display variable $\delta^{18}O$ signatures, but they have identical $\delta^{18}O$ values. This is inconsistent with recrystallization nor with isotopic exchange with host rocks during a long-lived metamorphic event (see also Eppel and Abart, 1997).

(5) The $\delta^{13}C$ values centered at 0–1‰ are entirely consistent with typical marine carbonates (Bach et al., 2011) and broadly fit with other Mesozoic, marine-related ophicalcite occurrences from the Alpine realm (Appendix DR2).

Hydrothermal and Syn-Tectonic Carbonation

Considering the large thickness (~10 m; Fig. 3A) and the large carbonate content of the ophicalcites, we can infer that seawater is an infinite isotopic reservoir in the fluid-rock interaction system. Hence, we can evaluate the precipitation temperature of calcite from seawater. Taking $\delta^{18}O_{SW} = 0‰$ and using the fractionation factor of Kim and O'Neil (1997), we obtain 90–105 °C, a range considerably higher than the typical temperatures of carbonate precipitation at present seafloor (~0–15 °C; Bach et al., 2011; Alt and Shanks, 2003) or measured at the Iberian margin (~19–44 °C; Agrinier et al., 1996; Schwarzenbach et al., 2013).

The remarkable isotopic homogeneity, i.e., homogeneous temperature, documented in this study compared to other ophicalcites (Appendix DR2) implies that carbonation occurred as a dramatic, sudden event, the mechanism of precipitation being

unknown to date. Serpentinite breccias, formed during exhumation and subsequent sedimentary reworking over exhumed mantle correspond to a high permeability zone above which basalts were emplaced and underwent syn-emplacement greenschist alteration (Fig. 4, stage I). Both the overlying massive and strongly altered basalts and the underlying serpentinite gouges correspond to a low-permeability zone. The influx of seawater-derived hydrothermal fluids in the high-permeability zone triggered carbonation. The mechanisms of heating and downward circulation of seawater are likely comparable to those described for ultramafic-hosted hydrothermal systems leading to black smoker-type mineralizations or carbonate chimneys (e.g., McCaig et al., 2007; Alt et al., 2018). In the regional context of mantle exhumation, a positive feedback occurred between fluid flow and the extensional reactivation of the detachment plane. Indeed, even if the amount of slip may have been limited, it enhanced dynamic permeability (stage II). Epidote veins in the basalts were re-opened and calcite veins formed in the serpentinites, all displaying orientations consistent with regional extension.

The present model contrasts with previous ones assuming that carbonation of serpentinized mantle occurs along the detachment plane during mantle exhumation or under static conditions at the seafloor in the absence of magma (e.g. Lost City hydrothermal field at MAR; Kelley et al., 2001). The coincidence of carbonation and magmatism along present-day fault zones is poorly constrained due to the lack of access to such outcrop. We propose that syn-tectonic carbonation along reactivated detachment segment in relationship with overlying basalts may be an important contribution to oceanic hydrothermal systems, including those leading to metal deposition, and may likely be more widespread than previously thought.

CONCLUSIONS

Syn-tectonic carbonation along the Jurassic Falotta detachment (Swiss Alps) resulted from the infiltration of hot seawater (~100 °C) into the high-permeability zone at the top of exhumed serpentinites. The homogeneity of isotopic compositions pleads for a sudden, short-lived fluid circulation. Extensional reactivation of the detachment plane, with limited slip during magma emplacement, was favored by fluid-related weakening, with a positive feedback between deformation-induced dynamic permeability and fluid influx.

ACKNOWLEDGMENTS

This work was funded through a grant from Petrobras to G. Manatschal and from the CNRS-INSU (CESSUR) to P. Boulvais. This work was improved by two anonymous reviewers and Laurent Jolivet. S. Picazo, P. Gautier, and K. Gallagher are thanked for fruitful discussions.

REFERENCES CITED

Agrinier, P., Cornen, G., and Beslier, M.O., 1996, Mineralogical and oxygen isotopic features of serpentinites recovered from the ocean/continent transition in the Iberia Abyssal Plain: Proceedings of the Ocean Drilling Program, Scientific Results, v. 149, p. 541–552, College Station, Texas, Ocean Drilling Program, https://doi.org/10.2973/odp.proc.sr.149.223.1996

Alt, J.C., and Shanks, W.C., 2003, Serpentinization of abyssal peridotites from the MARK area, Mid-Atlantic Ridge: Sulfur geochemistry and reaction modelling: Geochimica et Cosmochimica Acta, v. 67, p. 641–653, https://doi.org/10.1016/S0016-7037(02)01142-0.

Alt, J., Crispini, L., Gaggero, L., Levine, D., Lavagnino, G., Shanks, P., and Gulbransen, C., 2018, Normal faulting and evolution of fluid discharge in a Jurassic seafloor ultramafic-hosted hydrothermal system: Geology, v. 46, p. 523-526, https://doi.org/10.1130/G40287.1.

Bach, W., Rosner, M., Jöns, N., Rausch, S., Robinson, L.F., Paulick, H., and Erzinger, J., 2011, Carbonate veins trace seawater circulation during exhumation and uplift of mantle rock: Results from ODP Leg 209: Earth and Planetary Science Letters, v. 311, p. 242–252, https://doi.org/10.1016/j.epsl.2011.09.021.

Bernoulli, D., and Weissert, H., 1985, Sedimentary fabrics in Alpine ophicalcites, south Pennine Arosa zone, Switzerland: Geology, v. 13, p. 755–758, https://doi.org/10.1130/0091-7613(1985)13<755:SFIAOS>2.0.CO;2.

Bill, M., O'Dogherty, L., Guex, J., Baumgartner, P.O., and Masson, H., 2001, Radiolarite ages in Alpine-Mediterranean ophiolites: Constraints on the oceanic spreading and the Tethys-Atlantic connection: Geological Society of America Bulletin, v. 113, p. 129–143, https://doi.org/10.1130/0016-7606(2001)113<0129:RAIAMO>2.0.CO;2.

Boillot, G., et al., 1987, Tectonic denudation of the upper mantle along passive margins; a model based on drilling results (ODP Leg 103, western Galicia margin, Spain): Tectonophysics, v. 132, p. 335–342, https://doi.org/10.1016/0040-1951(87)90352-0.

Cannat, M., Sauter, D., Escartin, J., Lavier, L., and Picazo, S., 2009, Oceanic corrugated surfaces and the strength of the axial lithosphere at slow spreading ridges: Earth and Planetary Science Letters, v. 288, p. 174–183, https://doi.org/10.1016/j.epsl.2009.09.020.

Decarlis, A., Gillard, M., Tribuzio, R., Epin, M.E., and Manatschal, G., 2018, Breaking up continents at magma-poor rifted margins: A seismic vs. outcrop perspective: Journal of the Geological Society, https://doi.org/10.1144/jgs2018-041 (in press).

Desmurs, L., Manatschal, G., and Bernoulli, D., 2001, The Steinmann Trinity revisited: Mantle exhumation and magmatism along an ocean-continent transition: The Platta nape, eastern Switzerland, *in* Wilson, R.C.L., et al., eds., Non-Volcanic Rifting of Continental Margins: A Comparison of Evidence from Land and Sea: The Geological Society of London Special Publications, v. 187, p. 235–266, https://doi.org/10.1144/GSL.SP.2001.187.01.12.

Eppel, H., and Abart, R., 1997, Grain-stable isotope disequilibrium during fluid-rock interaction. 2: An example from the penninic-austroalpine tectonic contact in eastern Switzerland: American Journal of Science, v. 297, p. 707–728, https://doi.org/10.2475/ajs.297.7.707.

Froitzheim, N., and Manatschal, G., 1996, Kinematics of Jurassic rifting, mantle exhumation, and passive-margin formation in the Austroalpine and Penninic nappes (eastern Switzerland): Geological Society of America Bulletin, v. 108, p. 1120–1133, https://doi.org/10.1130/0016-7606(1996)108<1120:KOJRME>2.3.CO;2.

Früh-Green, G.L., Weissert, H., and Bernoulli, D., 1990, A multiple fluid history in Alpine ophiolites: Journal of the Geological Society, v. 147, p. 959–970, https://doi.org/10.1144/gsjgs.147.6.0959.

Gutzmer, J., Pack, A., Lüders, V., Wilkinson, J.J., Beukes, N.J., and van Niekerk, H.S., 2001, Formation of jasper and andradite during low-temperature hydrothermal

seafloor metamorphism, Ongeluk formation, South Africa: Contributions to Mineralogy and Petrology, v. 142, p. 27–42, https://doi.org/10.1007/s004100100270.

Kim, S.T., and O'Neil, J.R., 1997, Equilibrium and nonequilibrium oxygen isotope effects in synthetic carbonates: Geochimica et Cosmochimica Acta, v. 61, p. 3461–3475, https://doi.org/10.1016/S0016-7037(97)00169-5.

Kelley, D.S., et al., 2001, An off-axis hydrothermal vent field near the Mid-Atlantic Ridge at 30°N: Nature, v. 412, p. 145-149, https://doi.org/10.1038/35084000.

McCaig, A.M., Cliff, R.A., Escartin, J., Fallick, A.E., and McLeod, C.J., 2007, Oceanic detachment faults focus large volumes of black smoker fluids: Geology, v. 35, p. 935–938, https://doi.org/10.1130/G23657A.1.

MacLeod, C.J., et al., 2002, Direct geological evidence for oceanic detachment faulting: The Mid-Atlantic Ridge, 15°45′N: Geology, v. 30, p. 879–882, https://doi.org/10.1130/0091-7613(2002)030<0879:DGEFOD>2.0.CO;2.

Mehl, C., Jolivet, L., and Lacombe, O., 2005, From ductile to brittle: Evolution and localization of deformation below a crustal detachment (Tinos, Cyclades, Greece): Tectonics, v. 24, p. 1–23, https://doi.org/10.1029/2004TC001767.

Picazo, S., Manatschal, G., Cannat, M., and Andréani, M., 2013, Deformation associated to exhumation of serpentinized mantle rocks in a fossil Ocean Continent Transition: The Totalp unit in SE Switzerland: Lithos, v. 175–176, p. 255–271, https://doi.org/10.1016/j.lithos.2013.05.010.

Pinto, V.H.G., Manatschal, G., Karpoff, A.M., and Viana, A., 2015, Tracing mantle-reacted fluids in magma-poor rifted margins: The example of Alpine Tethys rifted

margins: Geochemistry Geophysics Geosystems, v. 16, p. 3271–3308, https://doi.org/10.1002/2015GC005830.

Schaltegger, U., Desmurs, L., Manatschal, G., Müntener, O., Meier, M., Frank, M., and Bernoulli, D., 2002, The transition from rifting to sea-floor spreading within a magma-poor rifted margin: field and isotopic constraints: Terra Nova, v. 14, p. 156–162, https://doi.org/10.1046/j.1365-3121.2002.00406.x.

Schwarzenbach, E.M., Früh-Green, G.L., Bernasconi, S.M., and Alt, J.C., 2013, Serpentinization and carbon sequestration: A study of two ancient peridotite-hosted hydrothermal systems: Chemical Geology, v. 351, p. 115–133, https://doi.org/10.1016/j.chemgeo.2013.05.016.

Weissert, J.H., and Bernoulli, D., 1984, Oxygen isotope composition of calcite in Alpine ophicarbonates: A hydrothermal or Alpine metamorphic signal?: Eclogae Geologicae Helvetiae, v. 77, p. 29–43, https://doi.org/10.5169/seals-165497.

FIGURE CAPTIONS

Figure 1. A: Map of the major paleogeographic and tectonic units in the Alps (after Schaltegger et al., 2002). B: Simplified geological map (after Desmurs et al., 2001) of the study area. C: Line-drawing photograph of the Falotta outcrop, southeastern Switzerland. Two decametric blocks of serpentinite have slipped down-slope.

Publisher: GSA
Journal: GEOL: Geology
DOI:10.1130/G45530.1

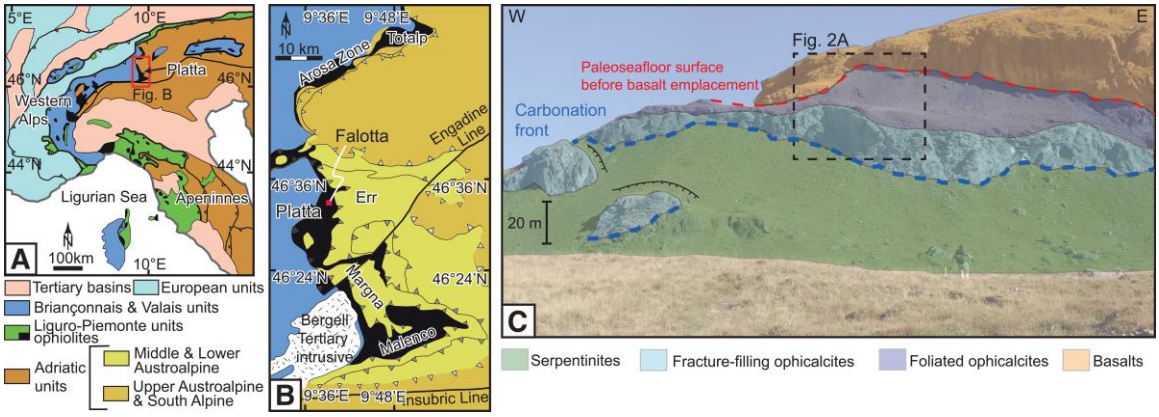

Figure 2. A: Schematic diagram illustrating the encountered lithologies at Falotta, southeastern Switzerland (not to scale). In the serpentinite and ophicalcite units: SL—serpentinite lenses; SB—serpentinite breccias. In the basalt unit: FH—foliated hyaloclastites; FB—foliated basalts; VB—veined basalts; MB—massive basalts. See text for details. B: Greenish serpentine vein crosscut by calcitic extensional veins (Cal EV) in a serpentinite lens (photograph from a sliding block). C: Thin-section photograph showing the greenschist alteration in the basalts [chlorite (Chl), epidote (Ep), quartz (Qtz) and albite (Alb)] sealed by calcite (Cal) in a vein. D: Thin-section of a foliated ophicalcite. Serpentine (serp) is replaced by calcite during fluid-assisted deformation forming a gouge (Serp+Cal). Spinel grains (Sp) are destabilized. Actinolite (Act) and hydro-andradite (h-An) grains accompany the alteration. E: Calcite pull-apart in foliated ophicalcites.

Publisher: GSA
Journal: GEOL: Geology
DOI:10.1130/G45530.1

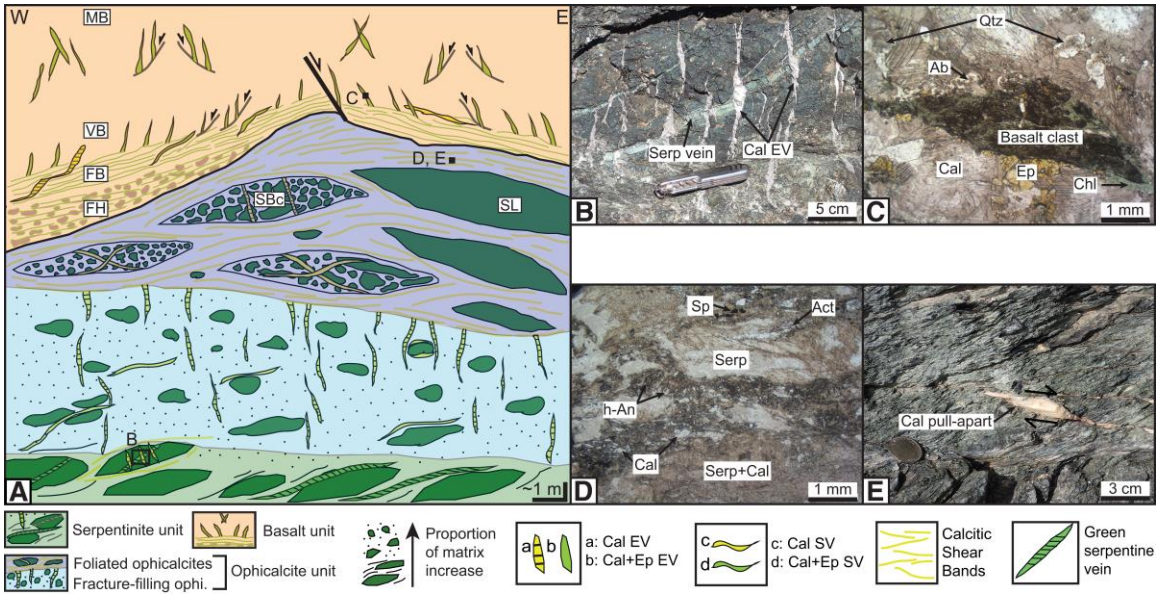

288

289

290 Figure 3. A: Synthetic log across the fossil detachment of Falotta, southeastern

291 Switzerland. B: Stereograms of vein poles (equal area, lower hemisphere, data number

292 N). See text for vein type abbreviations. C: $\delta^{18}O$ (VSMOW, Vienna Standard Mean

293 Ocean Water) and $\delta^{13}C$ (VPDB, Vienna Pee Dee Belemnite) versus depth.

294

Publisher: GSA
Journal: GEOL: Geology
DOI:10.1130/G45530.1

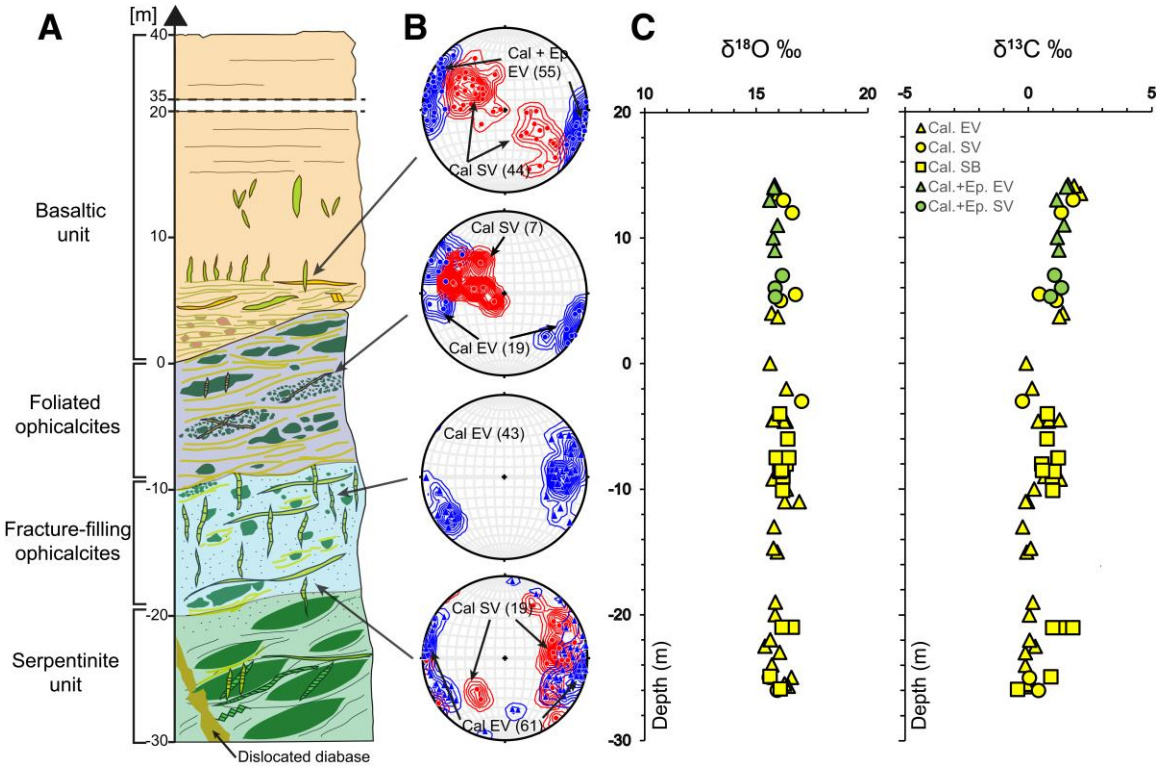

Figure 4. Model of carbonation (right-side sketch, I and II) in the context of magma-assisted mantle exhumation (left-side sketch). Carbonation is represented in blue (veins). Log scale, symbols and colors as in Figure 2. k—permeability. Adapted from Decarlis et al. (2018).

Publisher: GSA
Journal: GEOL: Geology
DOI:10.1130/G45530.1

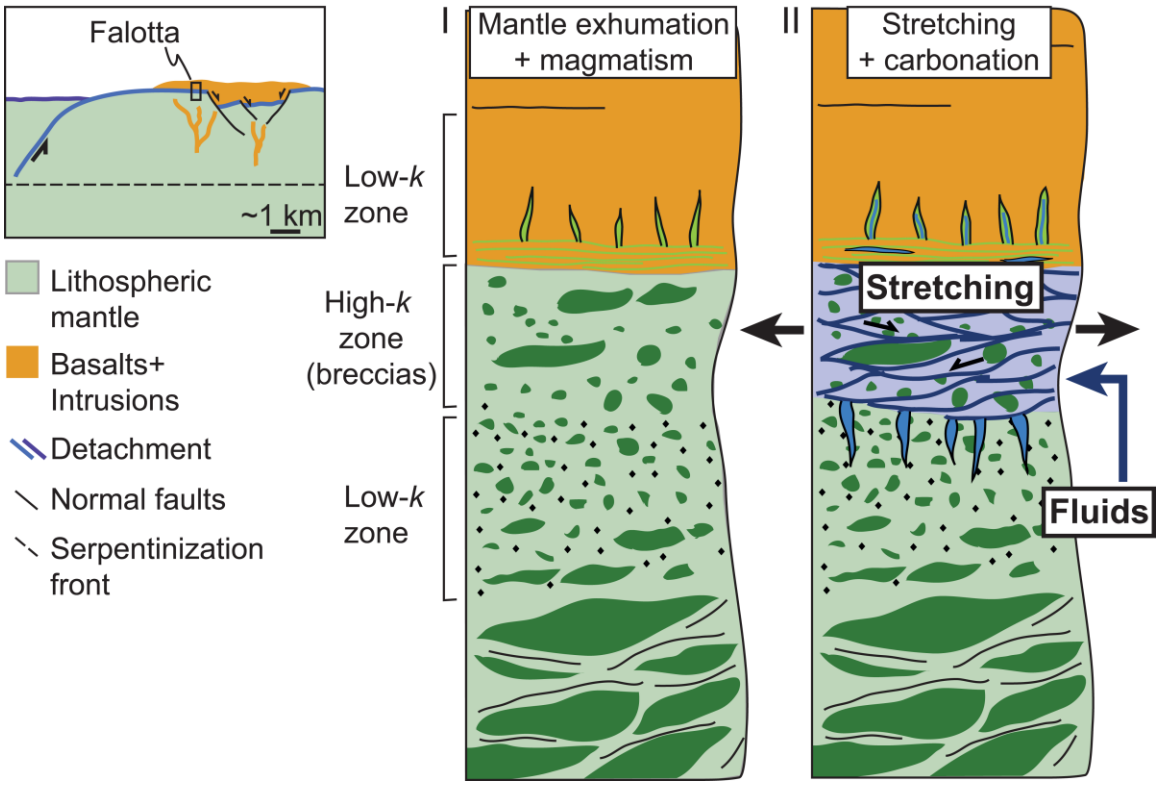

302

303 [1]GSA Data Repository item 2019xxx, xxxxxxxxxxxxxxxx, is available online at

304 http://www.geosociety.org/datarepository/2019/, or on request from

305 editing@geosociety.org.